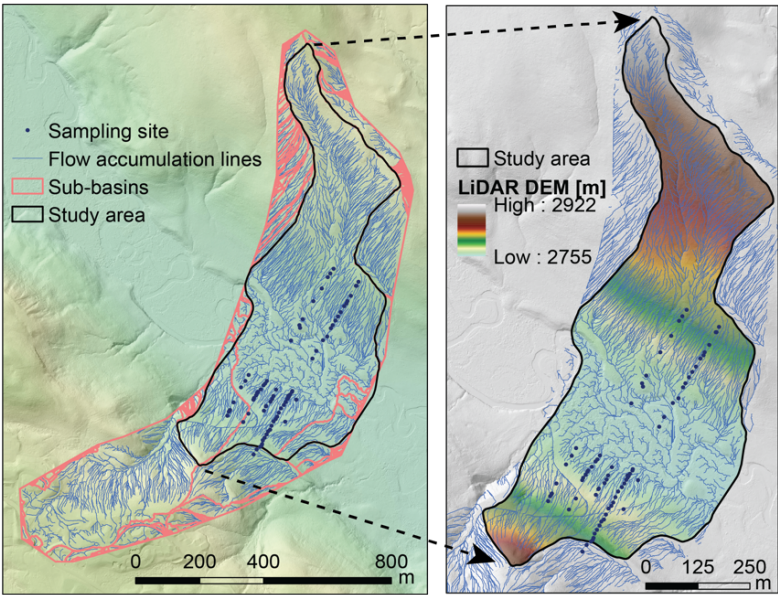


# Supplementary Information “Hybrid data-model driven prediction of soil thickness in a mountainous watershed”

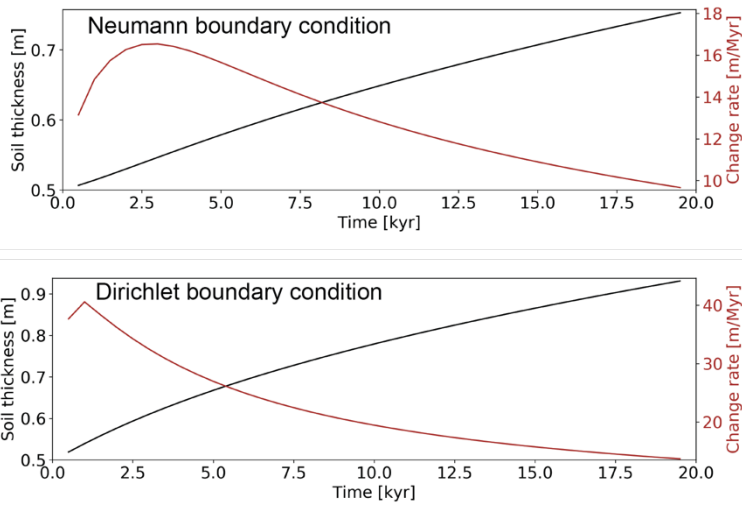
Qina Yan<sup>1</sup>, Haruko Wainwright<sup>1</sup>, Baptiste Dafflon<sup>1</sup>, Sebastian Uhlemann<sup>1</sup>, Carl I. Steefel<sup>1</sup>, Nicola Falco<sup>1</sup>, Jeffrey Kwang<sup>2</sup>, Susan S. Hubbard<sup>1</sup>

5 <sup>1</sup>Earth and Environmental Science Area, Lawrence Berkeley National Laboratory, Berkeley, CA., USA.  
<sup>2</sup> Department of Geosciences, University of Massachusetts Amherst, Amherst, MA, USA.

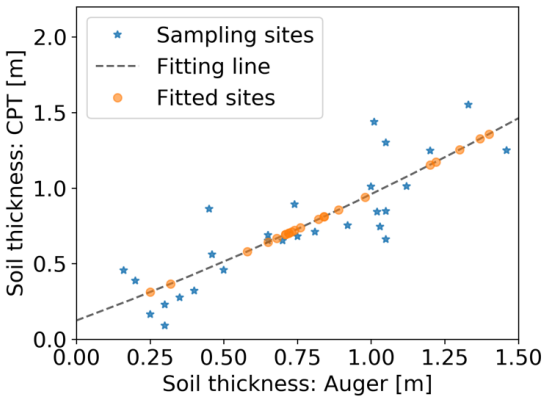
Correspondence to: Qina Yan ([qinayan@lbl.gov](mailto:qinayan@lbl.gov)); Haruko Wainwright ([HMWainwright@lbl.gov](mailto:HMWainwright@lbl.gov))



10 **Figure S1: Drainage area delineation.** The drainage areas are created by locating the pour points at the edges of the analysis window (where water would pour out of the raster), as well as sinks, then identifying the contributing area above each pour point.



15 **Figure S2: Spatial mean values of soil thickness evolution over time. The initial soil thickness is 0.5 m, and the initial elevation is the current DEM data. We tested two types of boundary conditions: both Neumann and Dirichlet. For the Neumann boundary condition, the surface transport fluxes around the edge is zero. For the Dirichlet boundary condition, we assume the elevation on the edge is constant and the same as the initial values.**



20 **Figure S3: Fitting the soil thickness of the CPT data using the auger data.**

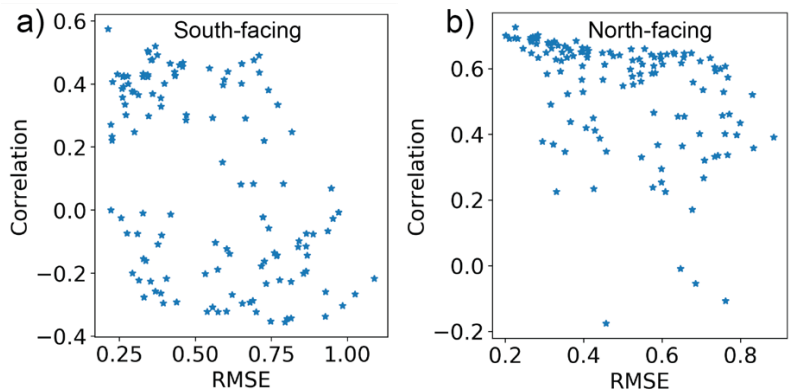


**Figure S4: Parameter calibrations for the hybrid model. The root-mean-square error (RMSE) and Pearson’s correlation between sampling and simulation results are calculated for the south-facing (a) and north-facing (b), respectively.**

**Table S1. A list of topographic variables for the correlation with soil thickness:**

Variable names	Explanation
Lidar_2018_Aspect_NEON	Topographical aspect computed at the original pixel resolution of 1m
Aspect_NEON_10m	Topographical aspect computed at a pixel resolution of 10m
Aspect_NEON_10m_x3	Topographical aspect computed at a pixel resolution of 10m and smoothed considering a 3x3-pixel moving window
Aspect_NEON_10m_x5	Topographical aspect computed at a pixel resolution of 10m and smoothed considering a 5x5-pixel moving window
Aspect_NEON_10m_x9	Topographical aspect computed at a pixel resolution of 10m and smoothed considering a 9x9-pixel moving window
C_unc	Uncertainty of the estimated leaf carbon content derived by airborne hyperspectral data (pixel resolution of 1 m)
C	Leaf carbon content derived by airborne hyperspectral data (pixel resolution of 1 m)
N_unc	Uncertainty of the estimated leaf nitrogen content derived by airborne hyperspectral data (pixel resolution of 1 m)
N	Leaf nitrogen content derived by airborne hyperspectral data (pixel resolution of 1 m)
CN_unc	Uncertainty of the estimated leaf carbon/nitrogen ratio derived by airborne hyperspectral data (pixel resolution of 1 m)
CN	Leaf carbon/nitrogen derived by airborne hyperspectral data (pixel resolution of 1 m)
chm_mosaic	Canopy height model (i.e., plant height) at 1 m pixel resolution

LMA	Leaf mass area derived by airborne hyperspectral data (pixel resolution of 1 m)
LMA_unc	Uncertainty of the estimated leaf mass area derived by airborne hyperspectral data (pixel resolution of 1 m)
LWC	Leaf water content derived by airborne hyperspectral data (pixel resolution of 1 m)
Curv_NEON_10m	Topographical curvature computed at a pixel resolution or 10m
Curv_NEON_10m_x3	Topographical curvature computed at a pixel resolution or 10m and smoothed considering a 3x3-pixel moving window
Curv_NEON_10m_x5	Topographical curvature computed at a pixel resolution or 10m and smoothed considering a 5x5-pixel moving window
Curv_NEON_10m_x9	Topographical curvature computed at a pixel resolution or 10m and smoothed considering a 9x9-pixel moving window
dsm_mosaic	Digital surface model at 1 m resolution
dsm_mosaic_10m	Digital surface model at 10 m resolution
dtm_mosaic	Digital terrain model at 1 m resolution
dtm_mosaic_10m	Digital terrain model at 10 m resolution
FlowAcc_NEON	Topographical flow accumulation computed at the original pixel resolution of 1m
FlowAcc_NEON_10m	Topographical flow accumulation computed at a pixel resolution of 10m
FlowAcc_NEON_10m_x3	Topographical flow accumulation computed at a pixel resolution of 10m and smoothed considering a 3x3-pixel moving window
FlowAcc_NEON_10m_x5	Topographical flow accumulation computed at a pixel resolution of 10m and smoothed considering a 5x5-pixel moving window
FlowAcc_NEON_10m_x9	Topographical flow accumulation computed at a pixel resolution of 10m and smoothed considering a 9x9-pixel moving window
NEON_mosaic_NDNI	Normalized difference nitrogen index computed from the airborne hyperspectral data
NEON_mosaic_NDVI	Normalized difference vegetation index computed from the airborne hyperspectral data
NEON_mosaic_NDWI	Normalized difference water index computed from the airborne hyperspectral data
NEON_mosaic_liq_water	Canopy water content estimated from the airborne hyperspectral data
SlopeDeg_NEON	Topographical aspect computed at the original pixel resolution of 1m
SlopeDeg_NEON_x3	Topographical slope in degree computed at a pixel resolution of 1m and smoothed considering a 3x3-pixel moving window
SlopeDeg_NEON_x9	Topographical slope in degree computed at a pixel resolution of 1m and smoothed considering a 9x9-pixel moving window
SlopeDeg_NEON_10m	Topographical slope in degree computed at a pixel resolution of 10m

SlopeDeg_NEON_10m_x3	Topographical slope in degree computed at a pixel resolution of 10m and smoothed considering a 3x3-pixel moving window
SlopeDeg_NEON_10m_x5	Topographical slope in degree computed at a pixel resolution of 10m and smoothed considering a 5x5-pixel moving window
SlopeDeg_NEON_10m_x9	Topographical slope in degree computed at a pixel resolution of 10m and smoothed considering a 9x9-pixel moving window
Srad_10m	Solar radiation computed at a pixel resolution of 10m.
TPI_NEON_10m_x3	Topographical position index computed at a pixel resolution of 10m and smoothed considering a 3x3-pixel moving window
TPI_NEON_10m_x5	Topographical position index computed at a pixel resolution of 10m and smoothed considering a 5x5-pixel moving window
TPI_NEON_10m_x9	Topographical position index computed at a pixel resolution of 10m and smoothed considering a 9x9-pixel moving window
TWI_NEON_10m	Topographical wetness index computed at a pixel resolution of 10m
TWI_NEON_10m_x3	Topographical wetness index computed at a pixel resolution of 10m and smoothed considering a 3x3-pixel moving window
TWI_NEON_10m_x5	Topographical wetness index computed at a pixel resolution of 10m and smoothed considering a 5x5-pixel moving window
TWI_NEON_10m_x9	Topographical wetness index computed at a pixel resolution of 10m and smoothed considering a 9x9-pixel moving window
UPslope_NEON_10m	local upslope drainage area computed at a pixel resolution of 10m
UPslope_NEON_10m_x3	local upslope drainage area computed at a pixel resolution of 10m and smoothed considering a 3x3-pixel moving window
UPslope_NEON_10m_x5	local upslope drainage area computed at a pixel resolution of 10m and smoothed considering a 5x5-pixel moving window
UPslope_NEON_10m_x9	local upslope drainage area computed at a pixel resolution of 10m and smoothed considering a 9x9-pixel moving window